# New calorimetric-structural aspects of temperature memory effect in hot rolled Cu-Zn-Al SMAs

G. VITEL, A. L. PARASCHIV[a], M. G. SURU[a], N. CIMPOESU[a], L.-G. BUJOREANU[a,*]
*"Axinte Uricariul" School, 707425 Scânteia, jud. Iaşi, Romania*
[a]*The "Gheorghe Asachi" Technical University from Iaşi, Bd. D. Mangeron 67, 700050 Iaşi, Romania*

Temperature memory effect (TME) is usually manifested by a kinetic stop during reverse transformation of thermally induced martensite to parent phase, after performing an incomplete heating in the previous thermal cycle, applied to a shape memory alloy (SMA). Technically TME causes the splitting of the endothermic peak corresponding to martensite reversion, on differential scanning calorimetry (DSC) thermograms. The present paper illustrates new manifestations of TME on DSC thermographs of hot rolled Cu-Zn-Al SMAs and discusses the accompanying structural changes observed by optical and scanning electron microscopy.

(Received July 17, 2011; accepted August 10, 2011)

*Keywords*: Temperature effect, Cu-Zn-Al shape memory alloy, Martensite population, Differential scanning calorimetry, Microstructure

## 1. Introduction

The main shape memory phenomena, observed in shape memory alloys (SMAs), are at the origins of thermal and mechanical memories, respectively. Thermal memory is represented by shape memory effect (SME) and by two way shape memory effect (TWSME) while mechanical memory is the attribute of pseudoelasticity (PE) which reaches isothermal complete shape recovery through superelasticity [1]. On these grounds shape memory applications have been divided into two main groups: Shape Memory and Superelastic Technologies (SMST), corresponding to thermal and mechanical memories, respectively. SMST developed as a prominent international organization affiliated to ASM, coordinating homonymous conferences that will reach their 9th edition this year, in November, in Hong Kong [2].

Besides SME, TWSME and PE, there are other less known secondary shape memory phenomena, characteristic for SMAs, such as: (i) dumping behaviour [3]; (ii) all round shape memory effect [4] and (iii) temperature memory effect.

The first systematic report on temperature memory effect (TME) is due to Mandangopal *et al.* who revealed it in Ni-rich NiTi SMAs, under the name of *thermal arrest memory effect (TAME)*. They pointed out that TAME consists in "remembering" the thermal arrest temperature applied during previous heating, by interrupting martensite reversion to parent phase (austenite), as a consequence of the locked-in transformation strain energy in the self-accommodation martensitic microstructure. The effect was insignificant in Cu-Zn-AI alloys as compared to Ni-Ti. The conclusion has been that, within each thermal cycle, TAME divided the total martensite "population" into two groups biased by different amounts of stored elastic energy: (i) a "primary population" of martensite which underwent no transformation in previous cycle (no reversion to austenite); (ii) a newly formed "secondary martensite" resulting from the austenite amount that formed during previous heating before the thermal arrest [5]. A schematization of TAME is shown in Fig. 1.

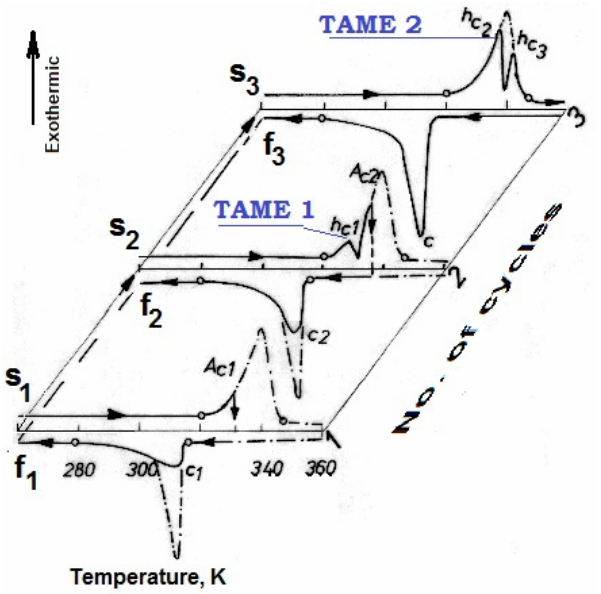


*Fig. 1. Schematic illustration of thermal arrest memory effect observed by Mandangopal et al. in $Ni_{50.5}Ti_{49.5}$ SMA [1, 5].*

In this case, the first thermal arrest was applied in cycle 1 at Ac1 and TAME 1 occurred in cycle 2, where second thermal arrest was applied at Ac2 and TAME 2 was observed in cycle 3.

Later, owing to the contribution of Zheng *et al.* the

property of TiNi SMAs to memorize the point of interruption of martensite to parent phase (austenite) transformation, from previous incomplete thermal cycle, upon heating, was designated as temperature memory effect (TME) [6].

Further studies performed on TiNi reported that TME can be revealed both on heating and cooling [7], even in a repeatable manner if the alloy was cold deformed over 12% [8] or if two way shape memory springs were subjected to a sequence of repetitious incomplete cycles with same arrested temperatures [9]. Recently Li *et al.* obtained *in situ* NiTi alloy composite materials with different density of dislocations, by controlling the ratio of the cold deformation in specimens with variable thickness due to their sinusoidal surfaces, which enabled the obtainment of a wide range TME [10].

In the case of TiNiCu SMAs a TME comprising up to four approximately equal spaced peaks were obtained in bars, by progressively decreasing interruption temperature during martensite reversion [11] and the same phenomenon was also observed in two way shape memory ribbons, thin films and wire [12]. The results have shown that the replacement of 20 at.% Ni with Cu prevents TME to occur during cooling in $Ti_{50}Ni_{30}Cu_{20}$ SMAs [13].

The number on incomplete thermal cycles "memorized" by TME could be increased up to 10 at $Ni_{47}Ti_{44}Nb_9$ SMAs, where the doubling of the temperature hysteresis of reverse transformation was obtained in this way [14] while at $Ti_{48}Ni_{17}Nb_{35}$ the TME induced by 30 incomplete thermal cycles upon heating persisted in the next 32 complete testing cycles [15].

Besides TiNi base SMAs, TME was also reported in Cu base alloys, even under multiple form, as it was observed in Cu-Al-Ni single crystals [16] and in Cu-Zn-Al polycrystals, in which case the effect was more obvious [17].

The present paper aims to discuss new calorimetric-structural aspects of TME, occurring in a polycrystalline Cu-Zn-Al SMA to which high density of dislocations was induced by hot-rolling and water quenching before being subjected to complex thermal cycling, during which the occurrence of newly formed martensite population will be suppressed due to low cooling rates applied after thermal arrest.

## 2. Experimental details

The experiments were performed on a Cu-15 Zn-6 Al (mass. %) SMA which was induction melted, cast, homogenized and hot forged as previously mentioned [18, 19]. The thickness of hot forged lamellas was further reduced, down to $5\times10^{-7}$ m, by hot rolling followed by instant water cooling, according to the schematized procedure illustrated in Fig. 2. A previous study demonstrated that the specimens under this condition are in fully martensitic state at room temperature (RT) [20].

The *calorimetric aspects* related to TME were analysed by differential scanning calorimetry (DSC), taking advantage of a previous report which emphasized a reversible martensitic transformation occurring in a Cu-Zn-Al SMA prepared according the same technological routine [21]. For this purpose, from hot-rolled water cooled specimens, fragments weighing less than $50\times10^{-6}$ kg were cut, without altering their thermomechanical histories. Subsequently, any marks of superficial corrosion were mechanically removed by careful grinding under water cooling. The fragments were subjected to thermal cycles comprising heating with 10K/min under Ar protective atmosphere and cooling either with air or liquid nitrogen, performed on a NETZSCH differential scanning calorimeter type DSC 200 F3 Maya, calibrated with Bi, In, Sn and Zn standards.

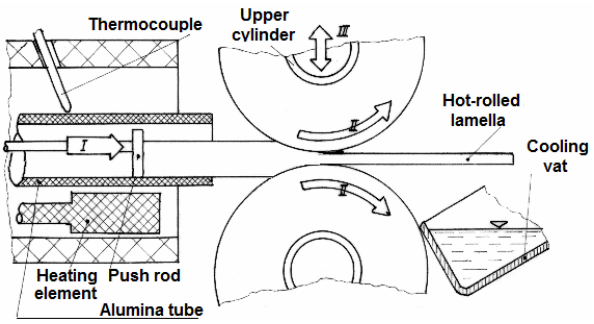


*Fig. 2. Schematized procedure for hot rolling and instant water cooling of Cu-15Zn-6Al (mass. %) SMA specimens: I-pushing action of the specimen; II-rotation of rolling cylinders; III-adjustment of rolling thickness.*

The DSC thermograms were recorded using corresponding correction curves and the results were evaluated with PROTEUS software.

The *structural aspects* related to TME were revealed by means of optical and scanning electron microscopy (OM and SEM, respectively). For this purpose hot rolled water cooled specimens were heat treated as it will be shown later and larger fragments were cut, with water cooling, and encapsulated into Mécaprex KM-U could mounting resign. After grinding with abrasive papers up to 2400 mesh and automatic polishing for 1.8 ks, on a Metkon FORCIPOL 1V machine, with 0.04 μ Alumine Suspension, the specimens were etched for 5 s with 30 % $HNO_3$ aqueous solution, after which alcohol and water neutralisations were applied. OM micrographs were recorded with a Meiji TECHNO microscope with video camera and QCapture software while SEM micrographs were obtained by means of a SEM—VEGA II LSH TESCAN microscope, coupled with an EDX—QUANTAX QX2 ROENTEC detector.

## 3. Experimental results and discussion

The typical DSC thermogram of the alloy in hot rolled water cooled state, further designated as A, is shown in Fig. 3.

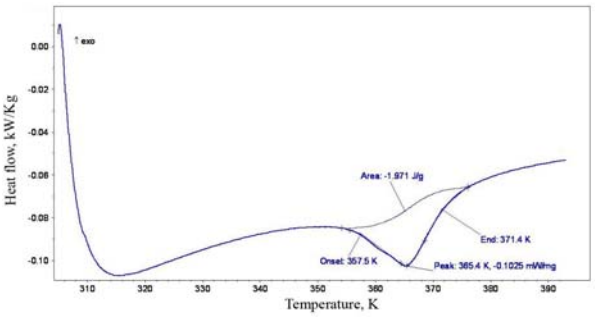


*Fig. 3. Typical DSC thermogram of hot rolled water cooled specimens in state A, revealing martensite reversion to parent phase (austenite) during heating.*

It is generally accepted that the endothermic peak occurring on DSC thermograms during the heating of a martensitic SMA corresponds to martensite reversion to parent phase [22], commonly named austenite [23].

Therefore it may be supposed that martensite (M) reverted to austenite (A) between $A_s$=357.5 K and $A_f$=371.4 K, being accompanied by a specific energy absorption $\Delta H^{M\rightarrow A} \cong 2$ kJ/kg. Based on these results, in order to reveal the structural aspects related to TME in the Cu-15 Zn-6 Al (mass. %) SMA under study heat treatments were applied as illustrated in Fig. 4.

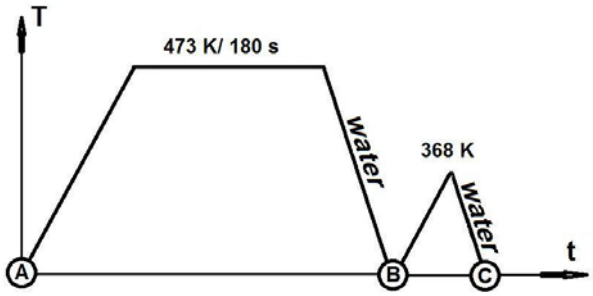


*Fig. 4. Heat treatment diagram of the three states of hot rolled water cooled specimens: A, B and C.*

It follows that state A corresponds to initial hot forged water cooled condition, state B to a fully thermally induced martensitic state while state C is representative for an incomplete heating. TME effects will be further analysed by OM and SEM on state C specimens.

The first thermal arrest (TA) temperature was 363 K and the corresponding calorimetric response, during two thermal cycles with uncontrolled air cooling is shown in Fig. 4. The cycling sequence was: 1. RT-313K-343K; 2. 343K-RT but due to air cooling the prescribed temperatures were not reached at the end of cooling.

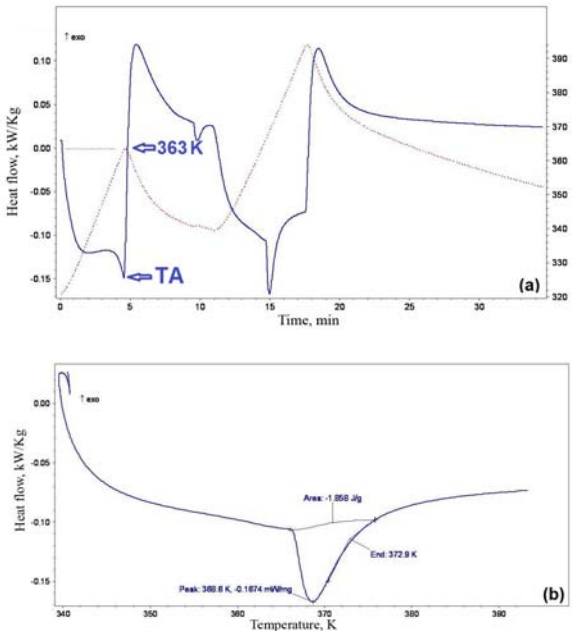


*Fig. 5. Calorimetric response of specimens in state A after a thermal arrest at 363 K: (a) heat flow and temperature variations in time; (b) DSC thermogram during heating after an incomplete thermal cycle.*

By comparing Fig. 4 with Fig. 5(b) it is noticeable that the first part of the endothermic peak is missing. This missing part would normally correspond to the reversion of newly formed martensite population, which occurred during the first cooling from the austenite islands that transformed before thermal arrest was applied. It is assumed that the peak noticeable in Fig. 5(b) corresponds to the reversion to austenite of only the primary untransformed population of martensite, which remained unchanged during previous incomplete heating [5].

In order to verify this assumption, to a new specimen the thermal arrest temperature was applied at 373 K and cooling end temperature was set at 298 K, in order to prolong the time for direct martensite formation from austenite, on cooling. The results are shown in Fig. 6.

It is obvious from Fig. 6(b) that the two peaks are complementary and that the reversion of the martensite population which should be newly formed during the cooling, that succeeded the incomplete heating cycle, could not be observed. Basically, both in Fig. 5(b) and 6(b) only the second part of the endothermic peak is noticeable, which suggests either that the newly formed martensite became stabilized and did not experience any reversion to austenite during subsequent heating or that it simply did not form due to too low cooling rate value.

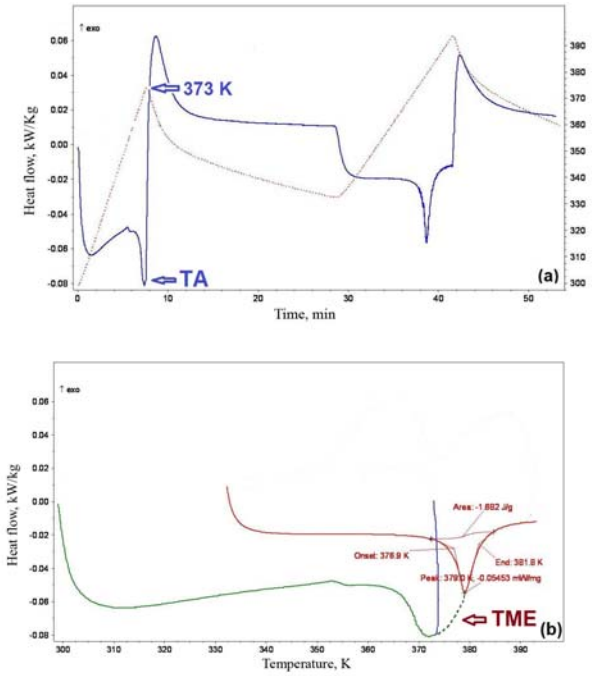


*Fig. 6. Calorimetric response of a specimen in state A after a thermal arrest at 373 K: (a) heat flow and temperature variations in time; (b) DSC thermogram during heating after an incomplete thermal cycle.*

Martensite stabilization during air cooling could have various reasons such as reciprocal blocking of differentially oriented martensite populations [20] or the transitory formation of bainite [24, 25] but no evidence was found in order to support this assumption. It follows that there was no newly formed martensite, and this represents a *new calorimetric aspect of TME*.

Considering that the formation of a new martensite population needs larger constant cooling rates, a new thermal arrest was applied, at 393 K, during complex thermal cycling performed with a rate of 10 K/ min, both on heating and cooling, according to Fig. 7.

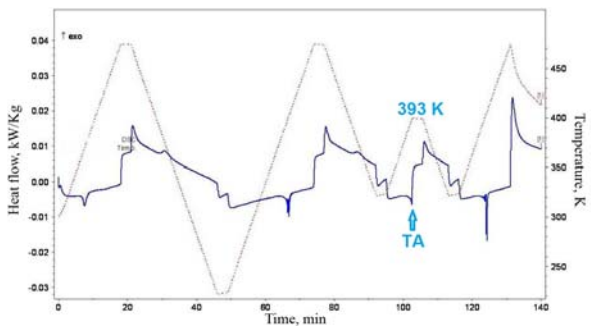


*Fig. 7. Calorimetric response of specimens in state A during complex thermal cycling with controlled cooling and thermal arrest at 393 K.*

The DSC thermogram of the incomplete thermal cycle and the subsequent heating is shown in Fig. 8.

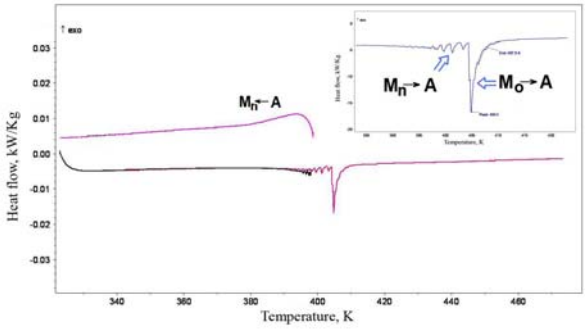


*Fig. 8. DSC thermogram of the incomplete thermal cycle and the subsequent heating with 10 K/ min, according to Fig. 7.*

In this case TME caused the appearance of endothermic peaks with two distinctive aspects: (i) a serrated region which could be associated with the reversion of newly formed martensite population ($M_n$); (ii) a sharp region associated with the reversion of old martensite population ($M_o$). So, the application of more intense cooling enabled the occurrence of the missing part of the complete endothermic peak, under the form of a serrated region.

In order to corroborate the calorimetric response with the structural changes, OM and SEM studies were performed on the specimen C, heat treated according to Fig. 4. The corresponding OM micrograph is shown in Fig. 9.

Two distinctive regions with different morphology were identified as representative for the newly formed martensite population, $M_n$. No similar regions were noticed when the thermal arrest was followed by uncontrolled air-cooling.

The presence of $M_n$ population was confirmed by SEM observations, as exemplified in Fig. 10, especially at large magnifications, such as in Fig. 10(b).

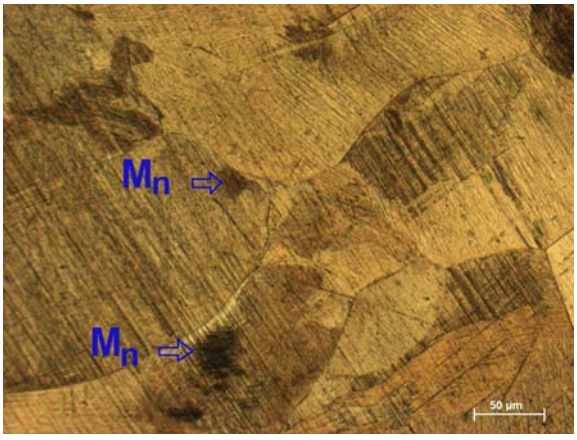


*Fig. 9. Typical OM micrograph of specimen C.*

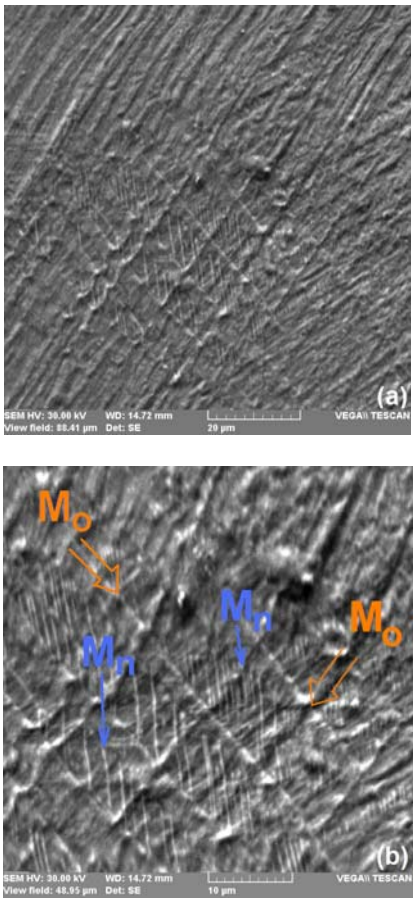


*Fig. 10. SEM micrograph of specimen C: (a) general aspect; (b) detail of newly formed martensite.*

The morphological differences between newly formed and old martensite, $M_n$ and $M_o$, respectively' are also emphasized by the difference in orientation between the two populations.

## 4. Conclusions

New calorimetric aspects of TME were revealed in the case of a hot rolled water cooled Cu-15 Zn-6 Al (mass. %) SMA subjected to a thermal cycle with incomplete heating and decreasing-rate air cooling. This procedure of complex thermal cycling prevented the forward martensitic transformation of the austenite areas, formed before thermal arrest, in such a way that no newly formed martensite ($M_n$) was noticeable since only old primary martensite ($M_o$) reverted to austenite within TME.

A constant cooling rate of 10 K/ min, applied after incomplete heating, enabled the occurrence of an endothermic serrated peak, corresponding to the reversion to austenite of newly formed martensite population.

The distinction between primary old and newly formed martensite was made on OM and SEM micrographs, owing to the different form and orientation of the two populations.

## References

[1] L. G. Bujoreanu, Intelligent Materials (in Romanian), Junimea, Iasi, 93 (2002).
[2] http://smst.asminternational.org/portal/site/smst/
[3] J. Van Humbeeck, Y. Liu, in Shape Memory Materials (T. Saburi ed.), Materials Science Forum, **327-3**, 331 (2000).
[4] D. Y. Li, X. F. Wu, T. Ko, Acta Metall Mater. **38,** 19 (1990).
[5] K. Madangopal, S. Banerjee, S. Lele, Acta Metall, Mater. **42,** 1875 (1994).
[6] Y. J. Zheng, L. S. Cui, Acta Metall Sin. **40,** 915 (2004).
[7] Z. G. Wang, X. T. Zu, S. Zhu, L. M. Wang, Mater Lett. **59,** 491 (2005).
[8] Yanjun Zheng, Juntao Li, Lishan Cui, Mater Lett. **63,** 949 (2009).
[9] H. J. Yu, Z. G. Wang, X. T. Zu, S. Z. Yang, L. M. Wang, J Mater Sci. **41,** 3435 (2006).
[10] Juntao Li, Yanjun Zheng, Lishan Cui, J Mater Eng Perform **19,** 998 (2010).
[11] X. M. He, J. H. Xiang, M. S. Li, S. W. Duo, S. B. Guo, R. F. Zhang, L. J. Rong, J Alloy Compd **422,** 338 (2006).
[12] Z. G. Wang, X. T. Zu, Y. Q. Fu, L. M. Wang, Thermochim Acta **428,** 199 (2005).
[13] Yong-Hua Li, Li-Jian Rong, Zhong-Tang Wang, Guang-Xia Qi, Cheng-Zhi Wang, J Alloy Compd **400,** 112 (2005).
[14] X. M. He, L. J. Rong, D. S. Yan, Y. Y. Li, Scripta Mater **53,** 1411 (2005).
[15] Daqiang Jiang, Lishan Cui, Yanjun Zheng, Xiaohua Jiang, J Mater Eng Perform. **19,** 1022 (2010).
[16] Javier Rodríguez-Aseguinolaza, Isabel Ruiz-Larrea, Maria Luisa Nó, Angel López-Echarri, José María San Juan, Acta Mater. **56,** 3711 (2008).
[17] Z. G. Wang, X. T. Zu, H. J. Yu, X. He, C. Peng, Y. Huo, Thermochim Acta **448**, 69 (2006).
[18] L. G. Bujoreanu, M. L. Craus, I. Rusu, S. Stanciu, D. Sutiman, J. Alloys Compd. **278**, 190 (1998).
[19] L. G. Bujoreanu, M. L. Craus, S. Stanciu, V. Dia, Mater. Sci. Technol. **16**, 612 (2000).
[20] L. G. Bujoreanu, N. M. Lohan, B. Pricop, N. Cimpoesu, J. Mater. Eng. Peform. **20**, 468 (2011).
[21] L.G. Bujoreanu, S. Stanciu, A. Enache, C. Lohan, I. Rusu, J. Optoelectron. Adv. Mater. **10**(3), 602 (2008).
[22] J. Spielfield, Mater. Sci. Eng. **A273–A275**, 639 (1999).
[23] C. M. Wayman, in Shape Memory Effects in Alloys (J. Perkins, ed.), Plenum Press, New York, 1–27 (1975).
[24] L. G. Bujoreanu, Mater. Sci. Eng. A **481–482**, 395 (2008).
[25] L. G. Bujoreanu, S. Stanciu, P. Bârsănescu, N. M. Lohan, in NM In: Advanced Topics in Optoelectronics, Microelectronics, and Nanotechnologies IV (P. Schiopu, C. Panait, G. Căruntu, A. Manea, eds.), Proc. SPIE Vol. 7297 SPIE, 72970B (2009).

*Corresponding author: lgbujor@tuiasi.ro